Available online at www.sciencedirect.com

ScienceDirect

Procedia Structural Integrity 2 (2016) 1047–1054

Structural Integrity Procedia

www.elsevier.com/locate/procedia

21st European Conference on Fracture, ECF21, 20-24 June 2016, Catania, Italy

Very high cycle fatigue of wrought magnesium alloy AZ61

U. Karr[a,*], A. Stich[b], H. Mayer[a]

[a]Institute of Physics and Materials Science, University of Natural Resources and Life Sciences, Vienna, Austria
[b]Audi AG, Ingolstadt, Germany

Abstract

Wrought magnesium alloys show a high strength to weight ratio, which makes them potentially attractive for load bearing components in automotive applications. Structural parts may be subjected to very high numbers of load cycles, and therefore the very high cycle fatigue properties of these materials are of great interest. Fatigue tests in laboratory air were carried out on wrought magnesium alloy AZ61 using ultrasonic fatigue testing equipment. The fatigue strength at 10^9 cycles is 98 MPa, which is 32% of the tensile strength. Fatigue cracks are predominantly initiated from slip bands at the surface. Near threshold fatigue crack growth was studied in ambient air and vacuum and showed a dominant influence of the environment. The threshold stress intensity amplitude at load ratio R=-1 is $K_{a,th}$ = 1.1 MPam$^{1/2}$ in air and 1.9 MPam$^{1/2}$ in vacuum. Crack propagation as small as 10^{-12} m/cycle could be documented in vacuum. Lowest growth rates observed in ambient air were about 10^{-10} m/cycle. In vacuum, a transgranular and ductile crack path is found for all investigated crack growth rates. Corrosive processes induced by ambient air cause a transition from ductile to brittle failure in the near threshold regime.

Keywords: Ultrasonic fatigue; Fatigue crack growth; Threshold stress intensity; Environmental influence; Magnesium alloy

1. Introduction

The low mass density and the high specific strength make magnesium alloys potentially interesting materials for applications where weight saving is an issue. Some applications already exist in automotive systems where the reduction of mass and consequential energy saving and emission reduction are most important aims in research and development. But still the application of magnesium alloys as load bearing components is limited. One reason is

* Corresponding author. Tel.: +43-1-47654-5174.
E-mail address: ulrike.karr@boku.ac.at

Copyright © 2016 The Authors. Published by Elsevier B.V. This is an open access article under the CC BY-NC-ND license (http://creativecommons.org/licenses/by-nc-nd/4.0/).

10.1016/j.prostr.2016.06.134

their greater sensitivity against environmental influences compared with aluminium alloys as the most frequently used lightweight materials.

These environmental influences are especially important, if the fatigue properties are considered. Several contributions have already been made to understand the fatigue behaviour of magnesium alloys in presence of chemically active environments. The fatigue properties in corrosive environments including saline solutions has been investigated by Mayer et al. (1999), Mutoh et al. (2008), Nan et al. (2008) and Unigovski et al. (2003). The results showed a significant reduction in fatigue life in saline solutions due to the formation of corrosion pits that induce crack initiation and premature failure at relatively low stress amplitudes.

However, chemical processes in magnesium alloys are already present in relatively mild environments, such as ambient air. The works of Kobayashi et al. (1997), Papakyriacou et al. (2002), Tokaji et al. (2009) and Uematsu et al. (2014) show that the presence of water vapour in ambient air can strongly accelerate fatigue crack growth and reduce the threshold stress intensity. It can be concluded that the damaging mechanism is hydrogen embrittlement caused by the humidity of ambient air.

The present work focuses on the high cycle fatigue (HCF) and very high cycle fatigue (VHCF) properties and near threshold fatigue crack growth of wrought magnesium alloy AZ61. Experiments were performed at cycling frequencies in the ultrasonic range. Particular attention was given to environmental influences acting on the fatigue life at very high numbers of load cycles by means of fractographic investigations.

2. Material and Method

2.1. Material

The material used in the present investigation was the as-extruded high purity magnesium alloy AZ61 hp. The chemical composition is (in weight %) 6.3 Al, 1.0 Zn, 0.2 Mn and balance Mg. Mechanical properties are: Ultimate tensile strength 302 MPa, Yield stress 224 MPa and Elongation 14 %. The mean grain size is approximately 5 µm.

Specimens were machined from as received, rectangular bars according to the specimen shapes, which are shown in Fig. 1 (specimen axis coincides with the extrusion direction). Edges in the centre regime of specimens used in fatigue tests were rounded (rounding radius about 0.5 mm). Then, they were ground parallel to the specimen's length axis with abrasive paper up to grade #600. Some specimens used for surface investigations were ground with abrasive paper up to grade #4000 and subsequently polished with alcohol-based aluminium oxide suspension up to a grain size of 0.04 µm to obtain a mirror like finish. Specimens used in fatigue crack growth (FCG) measurements were similarly polished up to a mirror like finish in order to optically observe crack growth. Furthermore, a single edge notch of 1 mm was introduced by electrical discharge machining.

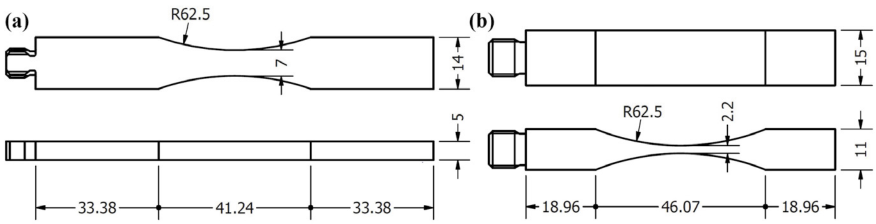

Fig. 1. Specimen shape used in (a) fatigue lifetime measurements; (b) in FCG measurements.

2.2. Experimental procedure

Lifetimes in the VHCF regime and near threshold fatigue crack growth were investigated using ultrasonic fatigue testing equipment developed at BOKU, Vienna. Performing an ultrasonic fatigue test, the specimen is stimulated to resonance vibrations in the range of frequencies close to 20 kHz. Thus the ends of the specimen vibrate in opposite directions resulting in a vibration node of maximum strain amplitude in its centre. Ultrasonic horn and specimen are designed appropriately in order to meet resonance condition. A comprehensive overview of ultrasonic fatigue testing results and a detailed description of the experimental procedure can be found in Mayer (2016).

Lifetime and FCG measurements were performed under fully reversed loading conditions (load ratio R=-1) in ambient air at 22°C and a relative humidity of 50%. In order to study environmental influences, additional FCG measurements in vacuum in the range of 1.1 to 1.5×10^{-5} mbar were carried out. The test setup for measurements in vacuum is shown in Fig. 2. Fatigue crack propagation was observed on the surface of the specimen using a CCD camera realising a magnification of approximately 300-fold. Numbers of cycles to propagate the crack by 70 - 100 µm each were evaluated to obtain crack propagation data.

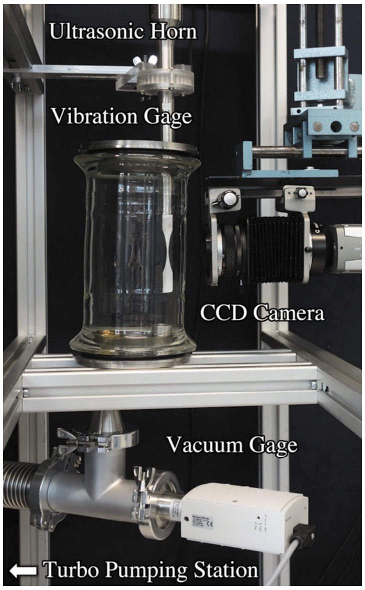

Fig. 2. Setup to perform ultrasonic fatigue experiments in vacuum.

3. Results

3.1. Lifetime measurements in ambient air

Fig. 3 shows the S-N curve of AZ61 measured at 20 kHz in ambient air. Numbers of cycles to failure range from 10^5 to 10^9. Failures were observed up to 2×10^9 load cycles, hence, the material shows no fatigue limit. The mean VHCF strength (i.e. 50% failure probability at 10^9 cycles) is 98 MPa. The ratio of VHCF strength and static strength is 0.32.

Fracture surface investigations revealed that the failure of all but two specimens originated from the surface. No inclusions or other stress raisers were found at the crack initiation sites suggesting that failure originated from slip bands.

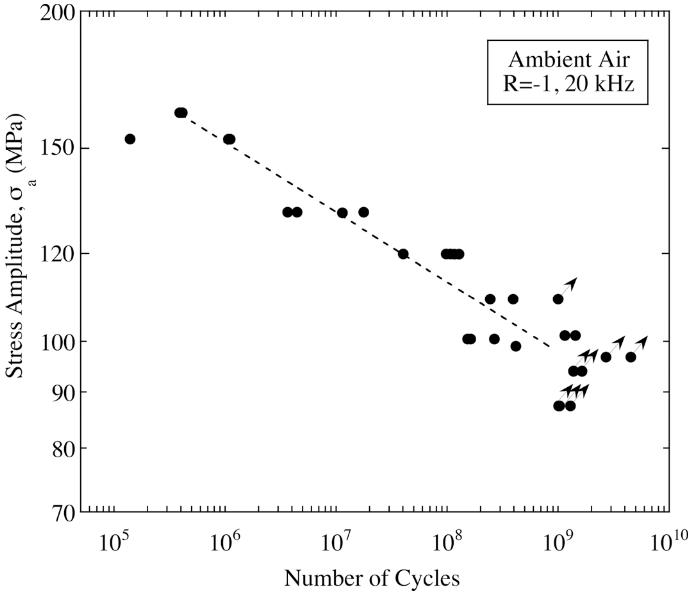

Fig. 3. S-N curve of AZ61, arrows indicate runout specimens.

Fig. 4 shows the crack initiation site of a specimen that was cycled at a stress amplitude of $\sigma_{□}$ = 101 MPa and failed after 1.2×10^9 load cycles. Close to the fracture surface, slip bands are visible which act as initiation sites for fatigue cracks.

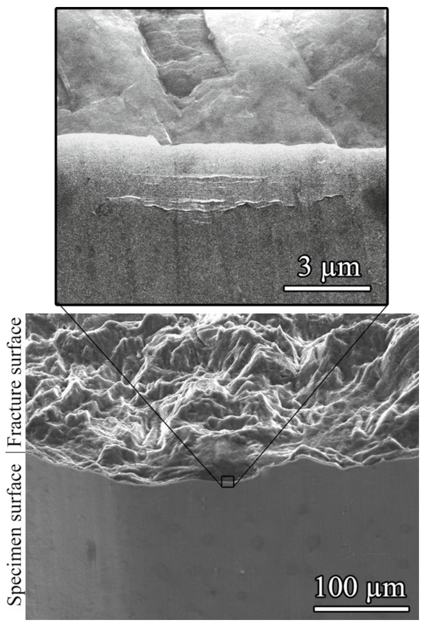

Fig. 4. Crack initiation site of a specimen that failed at a stress amplitude of σ_a = 101 MPa after 1.2×10^9 load cycles. Slip bands are visible on the specimen surface.

3.2. FCG measurements in ambient air and vacuum

The results of near threshold fatigue crack growth measurements at load ratio R=-1 in ambient air and in vacuum are shown in Fig. 5. Crack growth rates measured at ultrasonic frequencies are presented vs. the stress intensity amplitude, K_a. The investigated regime of fatigue crack growth rates is below 10^{-7} m/cycle.

Open circles in Fig. 5 show crack growth data measured in vacuum. The crack propagation curve may be divided into two regimes, above and below approximately 3×10^{-10} m/cycle, i.e., crack propagation greater or smaller than one burgers vector per cycle. At growth rates above 3×10^{-10} m/cycle and K_a greater 2.5 MPam$^{1/2}$, the da/dN vs. K_a curve can be approximated by a Paris law with an exponent of about 5. A most interesting fact for K_a smaller than 2.5 MPam$^{1/2}$ is the steadily decreasing crack growth curve. However, the crack propagation curve shows a very steep slope (exponent about 20). Minimum growth rates in vacuum in the range of 2×10^{-12} m/cycle were measured which means that crack propagation rates below one burgers vector per cycle could be experimentally verified. The specimen is stressed with 5×10^7 cycles to obtain a crack advance of approximately 0.1 mm. If no further crack growth is observed within minimum 5×10^7 cycles, it is assumed that the threshold stress intensity is reached. The threshold stress intensity amplitude measured in vacuum is $K_{a,th}$ = 1.9 MPam$^{1/2}$.

Crack growth rates measured in ambient air are presented with closed circles in Fig. 5. For crack growth rates in the range of 10^{-7} to 5×10^{-9} m/cycle, FCG rates in ambient air and in vacuum are in the same range of scatter. Thus, the same exponent of 5 may be used to approximate crack growth data using a Paris law. Below 5×10^{-9} m/cycle, the FCG curve in ambient air shows a plateau-like regime with a significantly reduced slope. An exponent slightly above 1 may be used to approximate data for stress intensity amplitudes between 1.5 and 4 MPam$^{1/2}$. Below 1.5 MPam$^{1/2}$, the crack growth curve becomes steeper again. Crack propagation stops when the threshold stress intensity amplitude of $K_{a,th}$ = 1.1 MPam$^{1/2}$ is reached. In contrast to vacuum, cracks propagate at a minimum rate of 10^{-10} m/cycle in air or they stop propagating.

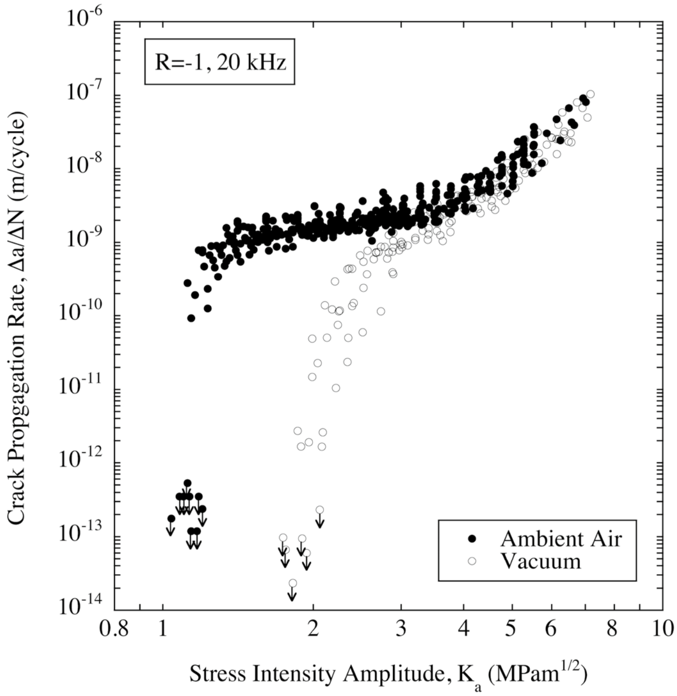

Fig. 5. Fatigue crack growth rates of AZ61 in ambient air and vacuum. Arrows indicate threshold stress intensities.

3.3. Fractography

Fig.6 shows fracture surfaces formed at different stress intensity amplitudes in ambient air and vacuum. Crack propagation direction is from left to right. Fractographic investigations reveal a transgranular crack path for both environments and for all investigated crack growth rates.

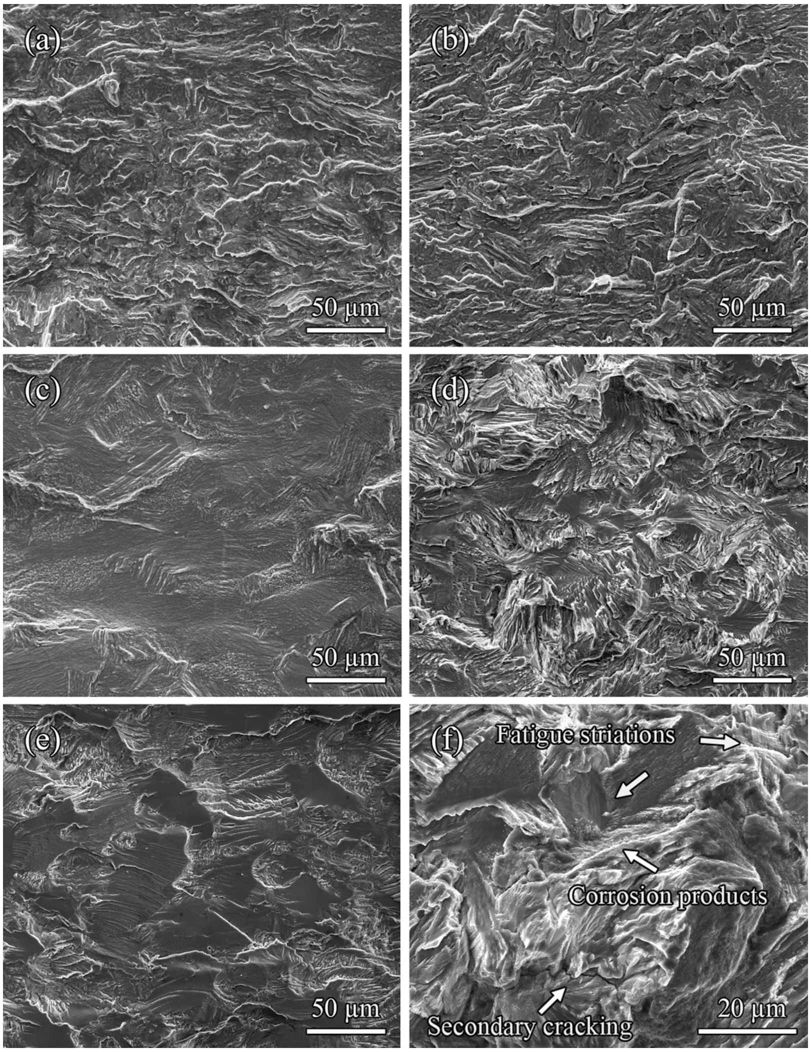

Fig. 6. Fracture surface formed (a) in vacuum at $K_a \approx 6.5$ MPam$^{1/2}$; (b) in ambient air at $K_a \approx 5.9$ MPam$^{1/2}$; (c) in vacuum at $K_a \approx 2.4$ MPam$^{1/2}$; (d) in ambient air at $K_a \approx 2.5$ MPam$^{1/2}$; (e) in ambient air at $K_a \approx 1.3$ MPam$^{1/2}$; (f) higher magnification of the fracture morphology formed in ambient air at $K_a \approx 2.5$ MPam$^{1/2}$.

Fracture surfaces formed at crack growth rates above 10^{-8} m/cycle are shown in Fig. 6a (vacuum) and Fig. 6b (ambient air). The fracture morphologies in ambient air and vacuum appear to be similar displaying a rather smooth and featureless stage II fatigue fracture surface.

Fracture surfaces formed at crack growth rates below 10^{-8} m/cycle are shown in Fig. 6c (vacuum) and Fig. 6d (ambient air). The fracture surface formed in vacuum (Fig. 6c) appears much smoother (compare Fig. 6a) featuring to an increasing extent deformation twins and fine granular areas. However, the fracture mode remains ductile and does not change with decreasing stress intensity amplitudes.

Fig. 6d shows a fracture surface formed in ambient air at crack growth rates in the plateau regime. A quasi-cleavage fracture mode exhibiting facets, corrosion products, secondary cracking and poorly developed fatigue striations are visible. These features are shown with higher magnification in Fig. 6f. The fracture surface formed in ambient air close to the threshold stress intensity is shown in Fig. 6e. With decreasing crack growth rates, the cleavage facets seem to enlarge leading to a smoother fracture morphology in the near threshold regime (compare Fig. 6d and 6e).

4. Discussion

The FCG curve in ambient air displays a pronounced plateau-like regime with almost constant growth rates of approximately 10^{-9} m/cycle. Fractographic studies reveal a transition from ductile to brittle failure exhibiting cleavage facets, secondary cracking, corrosion products and poorly developed fatigue striations. This change to a cleavage-like fracture mode can explain the acceleration of crack growth rates observed in ambient air. The cleaved facets, acting as cracks or voids ahead of the fatigue crack, advance the crack front considerably. Decreasing stress intensities coincide with increasing cleavage facets.

It has been generally acknowledged that ambient air acts as a corrosive environment inducing stress corrosion cracking in magnesium alloys. As a result of the present investigation, the threshold stress intensity amplitude is decreased to 58% of that in vacuum. A comparable acceleration of FCG rates has been observed by Uematsu et al. (2014) who studied the same material under controlled humidity. The authors showed that hydrogen generation results from anodic dissolution at the crack tip. Subsequent hydrogen diffusion into and embrittlement of the high stress field near the crack tip lead to accelerated crack growth rates.

The present fatigue crack growth experiments show that chemical processes caused by ambient air are present at ultrasonic frequencies, if the propagation rates are below approximately 10^{-8} m/cycle. However, the environmental influence diminishes at higher growth rates. In contrast, conventional fatigue crack growth experiments show environmental effects also at higher crack propagation rates. This difference may be well explained by the time dependency of chemical processes induced by humid air. The time governing process is in this case the diffusion of water molecules to the crack tip, where almost instantaneous reaction with the freshly formed surfaces can be assumed (Wei, 1980; Zhu et al., 2008a, b). This can lead to a frequency influence and lower crack propagation rates measured at higher cycling frequencies. Indeed, Zeng et al. (2012) and Kobayashi et al. (1997) report lower propagation rates in magnesium at higher frequencies and/or lower humidity content of the testing environment.

VHCF lifetimes in virtually defect free materials, such as AZ61, are dominated by the numbers of cycles required for crack initiation (Zimmermann, 2012). Fatigue cracks in AZ61 are created at the surface at slip bands without the presence of crack initiating inhomogeneities. Crack initiation and subsequent slow fatigue crack growth occurs under the embrittleing influence of air humidity. Environmental influences at ultrasonic frequency are found for K_a lower than 4 $MPam^{1/2}$. This corresponds to crack lengths smaller than 1 mm in S-N tests, which means that environmental influences exist for the major part of the fatigue life, if fatigue lifetimes are in the regime of high and very high numbers of cycles.

5. Conclusion

Very high cycle fatigue properties of wrought magnesium alloy AZ61 were investigated at 20 kHz cycling frequency using ultrasonic fatigue testing equipment. S-N data were measured up to 10^9 cycles in ambient air. FCG curves were measured in ambient air and vacuum in the near threshold regime. All tests were performed at R=-1. Following conclusions can be drawn:

1. Failures can occur at more than 10^9 cycles indicating the absence of a fatigue limit. Mean cyclic strength at 10^9 cycles is 32% of the static strength.
2. Fatigue cracks are initiated predominantly at the surface without any visible inclusions or stress raisers. The crack originates from slip bands.

3. Ambient air affects near threshold fatigue crack growth at ultrasonic frequencies. Threshold stress intensity amplitudes are $K_{a,th}$=1.1 MPam$^{1/2}$ in ambient air and 1.9 MPam$^{1/2}$ in vacuum. No influence is found above 3×10^{-9} m/cycle where the crack propagation rates in ambient air and vacuum are similar.
4. Under the influence of ambient air, the fracture mode changes from a typical stage II fatigue fracture to quasi-cleavage fracture in the near threshold regime.

References

Kobayashi, Y., Shibusawa, T., Ishikawa, K., 1997. Environmental effect of fatigue crack propagation of magnesium alloy. Materials Science and Engineering: A 234–236, 220-222.

Mayer, H., 2016. Recent developments in ultrasonic fatigue. Fatigue and Fracture of Engineering Materials and Structures 39, 3-29.

Mayer, H., Papakyriacou, M., Stanzl-Tschegg, S., Tschegg, E., Zettl, B., Lipowsky, H., Rösch, R., A Stich, 1999. Korrosionsermüdung verschiedener Aluminium- und Magnesium-Gußlegierungen. Materials and Corrosion 50, 81-89.

Mutoh, Y., Bhuiyan, M.S., Sajuri, Z., 2008. High cycle fatigue behavior of magnesium alloys under corrosive environment, Key Engineering Materials, pp. 131-146.

Nan, Z.Y., Ishihara, S., Goshima, T., 2008. Corrosion fatigue behavior of extruded magnesium alloy AZ31 in sodium chloride solution. International Journal of Fatigue 30, 1181-1188.

Papakyriacou, M., Mayer, H., Fuchs, U., Stanzl-Tschegg, S.E., Wei, R.P., 2002. Influence of atmospheric moisture on slow fatigue crack growth at ultrasonic frequency in aluminium and magnesium alloys. Fatigue Fract. Engng. Mater. Struct. 25, 795-804.

Tokaji, K., Nakajima, M., Uematsu, Y., 2009. Fatigue crack propagation and fracture mechanisms of wrought magnesium alloys in different environments. International Journal of Fatigue 31, 1137-1143.

Uematsu, Y., Kakiuchi, T., Nakajima, M., Nakamura, Y., Miyazaki, S., Makino, H., 2014. Fatigue crack propagation of AZ61 magnesium alloy under controlled humidity and visualization of hydrogen diffusion along the crack wake. International Journal of Fatigue 59, 234-243.

Unigovski, Y., Eliezer, A., Abramov, E., Snir, Y., Gutman, E.M., 2003. Corrosion fatigue of extruded magnesium alloys. Materials Science and Engineering A 360, 132-139.

Wei, R.P., 1980. Rate Controlling Processes and Crack Growth Response, in: Bernstein, I.M., Thompson, A.W. (Eds.), Hydrogen Effects in Metals. TMS, pp. 677-689.

Zeng, R., Han, E., Ke, W., 2012. A critical discussion on influence of loading frequency on fatigue crack propagation behavior for extruded Mg–Al–Zn alloys. International Journal of Fatigue 36, 40-46.

Zhu, X., Jones, J.W., Allison, J.E., 2008a. Effect of frequency, environment, and temperature on fatigue behavior of E319 cast aluminum alloy: Small crack propagation. Metall. Mater. Trans. A 39A, 2666-2680.

Zhu, X., Jones, J.W., Allison, J.E., 2008b. Effect of frequency, environment, and temperature on fatigue behavior of E319 cast aluminum alloy: Stress-controlled fatigue life response. Metall. Mater. Trans. A 39A, 2681-2688.

Zimmermann, M., 2012. Diversity of damage evolution during cyclic loading at very high numbers of cycles. Int. Mater. Rev. 57, 73-91.